

Structure and properties of graphene oxide/cellulose hybrid fibers via divalent metal ions treatment

Jisu Ryu · Jin Seong Lim · Seokhoon Ahn · Seong Mu Jo · Frank K. Ko ·
Joong Hee Lee · Jun Yeon Hwang 

Received: 1 August 2017 / Accepted: 24 October 2017 / Published online: 31 October 2017
© Springer Science+Business Media B.V. 2017

Abstract Cellulose hybrid fibers (CeHFs), hybridized via graphene oxide (GO) and metal ions (Ca^{2+}), are synthesized by dry-jet wet spinning. The synthesized GO- Ca^{2+} -CeHFs exhibit the tensile strength and the breaking elongation of 551 ± 37.5 MPa and $5.9 \pm 0.4\%$, respectively, while the GO/cellulose composite fibers (GO-CeFs) show the tensile strength of 403 ± 76.0 MPa and the elongation of $4.5 \pm 0.5\%$; thus, the GO- Ca^{2+} -CeHFs demonstrate improved mechanical properties over GO-CeFs by 37 and 31% in terms of tensile strength and elongation, respectively. These results are attributed to the metal ions that form a good interfacial interaction between the functional groups of cellulose and GO. In addition, the tensile strength of GO- Ba^{2+} -CeHFs is as high as 580 ± 25 MPa, which is induced by the difference in

the ionic radius. Therefore, the high mechanical properties of the synthesized cellulose-based fibers have the potential to be used as sustainable alternative to the synthetic fibers used in the industrial applications.

Keywords Nano hybrid materials · Cellulose fibers · Graphene oxide · Metal ion · Mechanical properties

Introduction

The increasing economic growth and the lack of sustainable materials and environmental concerns have led to the utilization of new materials from natural resources. Cellulose, one of the most abundant biomass on the earth, is biodegradable and environmentally friendly. Therefore, cellulose-based fibers have been gaining considerable attention and are widely used in clothing, tire cords, interior materials for automobile, and other industrial applications (Wu and Farnood 2015; Siró and Plackett 2010; Zhao et al. 2007). However, the mechanical properties of the cellulose fibers are noticeably lower than that of the synthetic fibers; furthermore, their production costs are prohibitively high which limits their industrial application (Unterweger et al. 2014; Mohanty et al. 2000). To overcome these issues, carbon materials (e.g. graphene, carbon nanotube, and carbon fiber) are

J. Ryu · J. S. Lim · S. Ahn · S. M. Jo · J. Y. Hwang (✉)
Institute of Advanced Composite Materials, Korea
Institute of Science and Technology (KIST) Korea,
Chudong-ro 92, Bongdon-eup, Wanju-gun,
Jeonbuk 55324, South Korea
e-mail: Junyeon.Hwang@kist.re.kr

J. Ryu · J. H. Lee (✉)
Department of BIN Convergence Technology, Chonbuk
National University, Baekje-daero 567, Dukjin-gu,
Jeonju-si, Jeonbuk 54896, South Korea
e-mail: jhl@chonbuk.ac.kr

F. K. Ko
Advanced Materials and Process Engineering Laboratory,
University of British Columbia, Vancouver, BC, Canada

used as fillers for the cellulose fibers matrix (Wang et al. 2011; Domun et al. 2015). Among the carbon materials, graphene is considered as promising filler since it exhibits exceptional mechanical, electrical and thermal properties within the confines of 2-dimensional (2D) layer (Geim and Novoselov 2007; Zhu et al. 2010; Stankovich et al. 2006). Graphene oxide (GO), which is oxygenated graphene, is thermodynamically stable than graphene and possesses oxygen functional group; thus, it can be easily dispersed and combined with the cellulose matrix (Dreyer et al. 2010). The GO-reinforced cellulose composites have been extensively reviewed to study the effects of GO for several applications including electronic devices, sensors, energy storages, ultra-lightweight materials, etc. (Wang et al. 2012; Yadav et al. 2013; Feng et al. 2012; Shi et al. 2014).

The interfacial bonding between the filler and the matrix is the key factor for the properties of composite materials. Poor interfacial bonding results in low mechanical properties due to the presence of gaps between the filler and the matrix (Terzopoulou et al. 2015). Recently, the development of a nano-hybrid material that exhibits drastically different properties has attracted great interest. Therefore research into the development of coupling agents (e.g. metal ions) as the 3rd component has been carried out in order to overcome the low interfacial bonding between two different materials (Li et al. 2015; Xu et al. 2013; Lee and Wang 2006). The remarkable observation by cross-linking on the bacterial cellulose has recently been reported (Wang et al. 2017; Yang et al. 2017). The enhanced interfacial bonding between two different materials can be attributed to the 3rd component of the nano-hybrid material. Since the 3rd component improves the interfacial bonding at a nanoscale level, nano-hybrid materials with various properties are realized through the method of interface control. Therefore, the nano-hybrid materials can be the potential alternative to the synthetic fibers for many industrial applications such as automobiles, aircrafts, and constructions, and bio-nanocomposites (Liu et al. 2012; Li et al. 2013; Charleux et al. 2015; Huang et al. 2015).

In this study, we show an environmentally friendly method to fabricate GO/cellulose fibers (GO–CeFs) by incorporating GO into the cellulose matrix using N-methylmorpholine-N-oxide (NMMO) based solvent. Likewise, metal ions are introduced as the 3rd

component for the GO–CeFs in order to enhance the interfacial adhesion between the cellulose and GO (GO/cellulose hybrid fibers; GO–CeHFs). The positive effect of the metal ions to the interaction between GO and the cellulose is investigated in terms of structure related mechanical properties of the GO–CeFs.

Experimental

Materials

The wood pulp (Buckeye, V-60) was used to fabricate the cellulose fibers. The wood pulp (α -cellulose content of 94% and degree of polymerization of 855) was dissolved in the N-methylmorpholine-N-oxide (NMMO) solvent (BASF, Germany). The n-propyl gallate (PG) was purchased from Sigma–Aldrich, USA. For the preparation of the GO, natural graphite flake with a purity of 99% was supplied by Alfa Aesar, USA. Calcium chloride (CaCl_2) and magnesium chloride (MgCl_2), barium chloride (BaCl_2), Copper II chloride (Cu(II)Cl_2), iron II chloride (Fe(II)Cl_2) were also used from Sigma–Aldrich, USA for the post-treatment of fibers.

Fabrication of CeFs and GO–CeFs

To prepare a spinning dope, 50% NMMO aqueous solvent was evaporated under a reduced pressure (to increase its concentration up to 86.7%. After the wood pulp was dried at 120 °C for 4 h, they were mixed with the prepared 87.6% NMMO solvent. The PG of 1 wt% was added into the dope as an antioxidant to prevent an oxidative decomposition during the dissolution. The mixture was stirred for 10 min before placing in an oil bath at 120 °C for 40 min under vacuum. In the preparation of the GO–CeFs, 0.2 wt% of the GO to cellulose ratio was added to the 50% NMMO solution before increasing its concentration to 86.7%. GO was prepared using a modified Hummers methods (Hummers and Offerman 1958). The solution of GO–CeFs was fabricated in the same way as that for the production of CeFs.

The CeFs and GO–CeFs were synthesized by dry-jet wet spinning with a 10 cm distance between the spinning nozzle and coagulation bath at 105 °C. The fabricated fibers were wound after passing through the coagulation and washing bath. Wound fibers were

immersed in the de-ionized water for 24 h to remove any NMMO residue before drying at room temperature for 24 h.

Fabrication of GO-CeFs

Fabricated CeFs and GO–CeFs were immersed in 0.1 M CaCl_2 solutions for 30 min. Afterwards, the CeFs and GO–CeFs were washed using the di-ionized water and then dried out thoroughly at 50 °C under tension. Post-treatment using other metal chloride was performed in the same way as described above mentioned.

Characterization

Raman spectrum was acquired using a LabRAM HR (Horiba, Japan) with laser wavelength of 514 nm to confirm the presence of GO. The mechanical properties of the fibers were determined using the FAVIMAT + single-fiber tester (Textechno, Germany). The tests were performed at a gauge length of 25 mm and a cross-head speed of 2 mm/min. In addition, liner densities of GO/Cellulose with ion treatment fibers measured by vibroscope attached to the FAVIMAT + following the ASTM D1577 (2012) procedure. Transmission electron microscopy (TEM) (Titan, FEI, USA) was used to investigate the morphology of GO in the cellulose fibers. Samples for TEM analysis were prepared by the ultra-microtome (PT-PC PowerTome, RMC, USA) and mounted on the 300-mesh lacey-carbon copper-grid (Ted pella, USA). Energy dispersive spectroscopy (EDS) (Super-X EDX, Bruker, Germany) analysis was performed by a 4-silicon drift detector system to determine their elemental compositions. The introduced surface metal ions and functional groups were investigated by x-ray photoelectron spectroscopy (XPS) (K-Alpha, Thermo Fisher Scientific, USA).

Results and discussion

Comparison of CeFs and GO–CeFs

Figure 1 shows the photographs of the CeFs and GO–CeFs. The photographs indicated that the white CeFs darkens by the addition of GO (Tian et al. 2014).

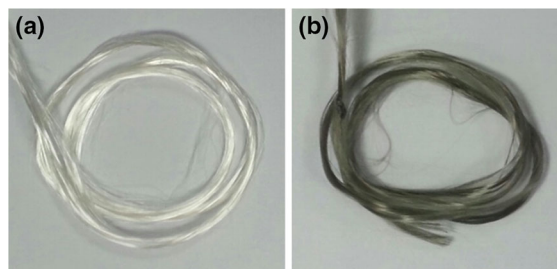


Fig. 1 Optical photographs of **a** CeFs and **b** GO–CeFs

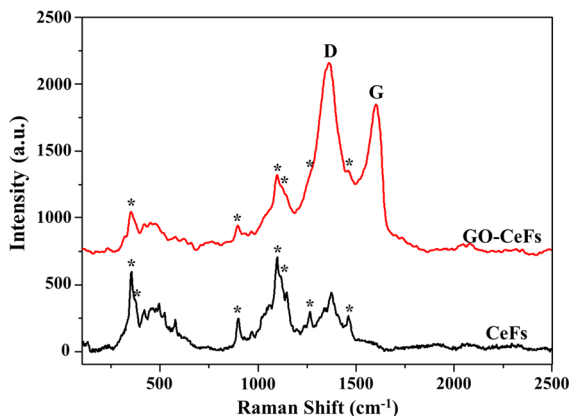


Fig. 2 Raman spectra of CeFs and GO–CeFs

Raman spectroscopy was used to investigate the existence of GO in the GO–CeFs. As shown in Fig. 2, both CeFs and GO–CeFs exhibit the Raman spectra in the range of 200 to 1250 cm^{-1} ; indicating characteristic bands from cellulose II (Zhbakov et al. 2002). The two main peaks around 1350 cm^{-1} and 1580 cm^{-1} in the GO–CeFs correspond to the D-band (associated to disorder or defect by oxidation of sp^2 carbon bonds) and G-band (arising from the in-plane vibration of sp^2 carbon bonds), respectively (Kudin et al. 2008).

The de-convoluted XPS analysis was applied to determine the surface functional groups of CeFs and GO–CeFs (Fig. 3). The $\text{C}1\text{ s}$ spectrum of CeFs presented in Fig. 3a represents three different functional groups. The major peak at about 284.6 eV is attributed to the C–C bonding. The peaks at about 285.6 and 286.7 eV correspond to the C–OH and C–O–C bonding, respectively (Belgacem et al. 1995). Figure 3b showed the $\text{C}1\text{ s}$ spectrum of GO–CeFs. Compared to the $\text{C}1\text{ s}$ spectrum of CeFs, two additional peaks are shown: $-\text{C}=\text{O}$ (~ 288.2 eV)

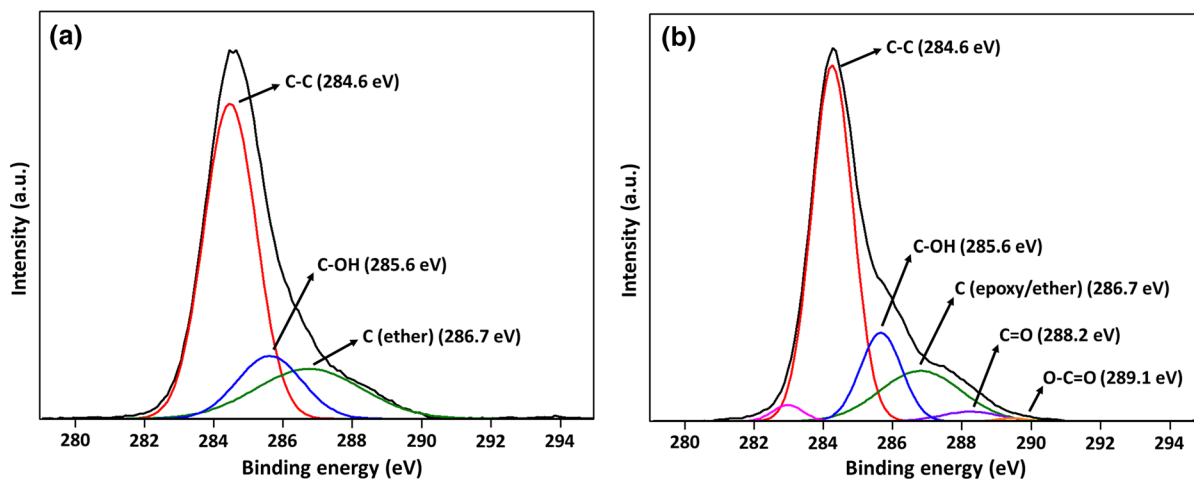


Fig. 3 De-convoluted Cls XPS spectra of **a** CeFs and **b** GO–CeFs

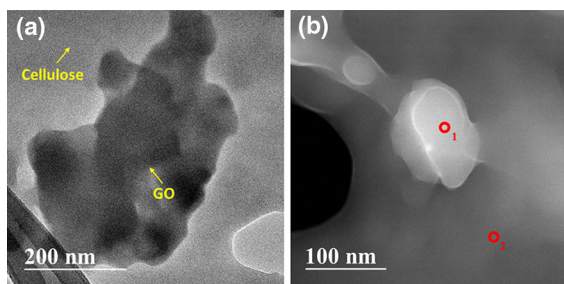


Fig. 4 **a** TEM BF images and **b** STEM HAADF images of GO–CeFs

and O–C=O (~ 289.1 eV) bonding. These two peaks were generated by the GO (Chen et al. 2014).

The morphology of GO in the cellulose was examined by TEM. The bright field (BF) TEM image shows the typical nanostructure of GO in the cellulose (Fig. 4a). Figure 4b shows the scanning transmission electron microscopy (STEM) image of the high angle annular dark field (HAADF) detector with EDS point profile of GO–CeFs. From the atomic percentage data of C–K and O–K edge in Table 1, the compositions of the nanostructure (point 1) indicate high atomic proportion of carbon and oxygen compared to the

Table 1 Carbon and oxygen atomic percentage data from the characteristic K-edge of EDS point profile analysis

	Point 1	Point 2
at.% of C	93.8	78.6
at.% of O	4.0	11.1

cellulose (point 2). Thus, it is reasonable to believe that the nanostructure is GO due to the remarkable oxygenated functional groups of GO in comparison with the cellulose.

The typical tensile stress–strain curves of CeFs and GO–CeFs are presented in Fig. 5. It can be seen that the tensile strength of GO–CeFs 403 ± 76.0 MPa, which is 11% higher than that of the CeFs (362 ± 46.6 MPa). Although the tensile strength of GO–CeFs is higher, its breaking elongation ($4.5 \pm 0.5\%$) is 33% lower than that of the CeFs ($6.0 \pm 0.6\%$).

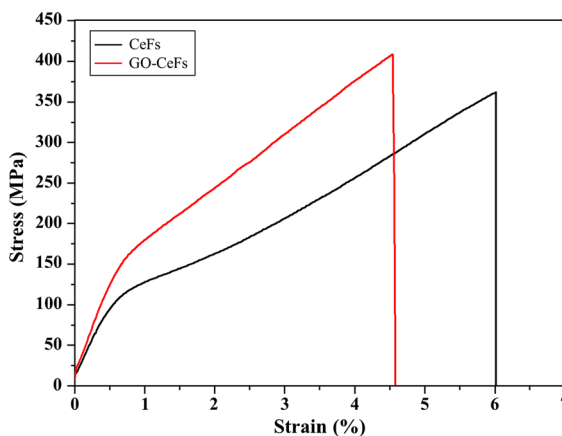


Fig. 5 Stress-strain curves of CeFs and GO–CeFs

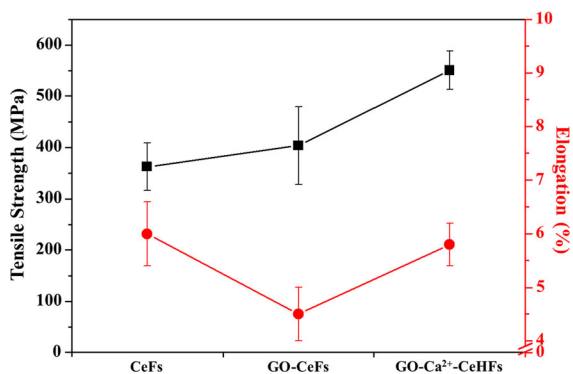


Fig. 6 Tensile strength and elongation of CeFs, GO-CeFs and GO-Ca²⁺-CeHFs

The effect of the metal ions post-treatment for the GO-CeFs

To further improve the mechanical properties of the GO-CeFs, metal ions (Ca²⁺) were used to improve the interfacial bonding between the functional groups of GO and the cellulose. Figure 6 shows the mechanical properties of CeFs, GO-CeFs and GO-Ca²⁺-CeHFs. The tensile strength of GO-Ca²⁺-CeHFs (551 ± 37.5 MPa) increased about 37% over that of the GO-CeFs. Furthermore, the elongation of GO-Ca²⁺-CeHFs increased up to 5.9 ± 0.4%, which is comparable to the breaking elongation of CeFs. This can be attributed to the van der Waals interactions or electrostatic interactions between the oxygenated functional groups of GO, cellulose and metal ions (Öztürk et al. 2009; Kramar et al. 2014).

The morphology of GO/Cellulose composite fiber and GO-Ca²⁺-CeHFs was shown at Fig. 7. The diameters of both samples are around ~ 10 μm,

which means the ion treatment did not affect on the surface and morphological configuration. The Linear density and diameters of ion-treatment fiber are presented in Table 2. From the measured values, there were no significant change of the linear densities and diameters after ion treatment.

TEM EDS mapping was carried out to observe the distribution of atoms in the GO-Ca²⁺-CeHFs to confirm that the metal ions affect the interfacial bonding between GO and cellulose (Fig. 8). Figure 8a shows the STEM HAADF image of the GO-CeFs which confirms the existence of nanometer-sized GO on the cellulose fiber. In Fig. 8b and 8c, the GO region shows slightly higher concentrations of carbon and oxygen elements than that in the cellulose region. Thus, it is confirmed that the nanoparticle shown in the TEM image (Fig. 4, Table 1) is indeed GO. Figure 8d depicts the distribution of calcium (Ca) elements showing denser distribution of Ca within the GO region. Therefore, it is observed that Ca ions (Ca⁺) distribution led to more densely packed interface between GO and cellulose.

In order to verify the Ca²⁺ distribution in the hybrid fibers, the XPS analysis was applied on the surface functional groups of calcium ion bonding between GO/Cellulose fiber. The Ca spectrum of GO-Ca²⁺-CeHFs presented in Fig. 9. The peaks at about 346.8 and 350.5 eV correspond to the Ca 2p_{3/2} and Ca 2p_{1/2} bonding. It revealed that Ca is well distributed after ion treatment in the GO-Ca²⁺-CeHFs sample.

Post-processing treatments using metal ions from Group 2 and Period 4 were carried out in order to determine their degree of improvement to mechanical properties (Fig. 10). Figure 10a represents the tensile strength and elongation results from the samples

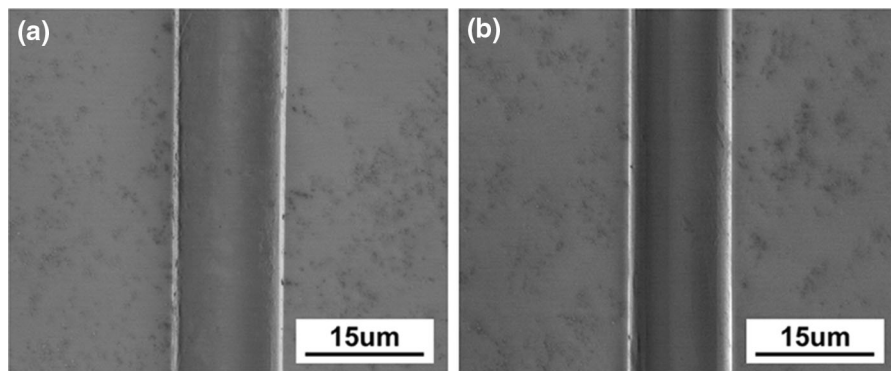
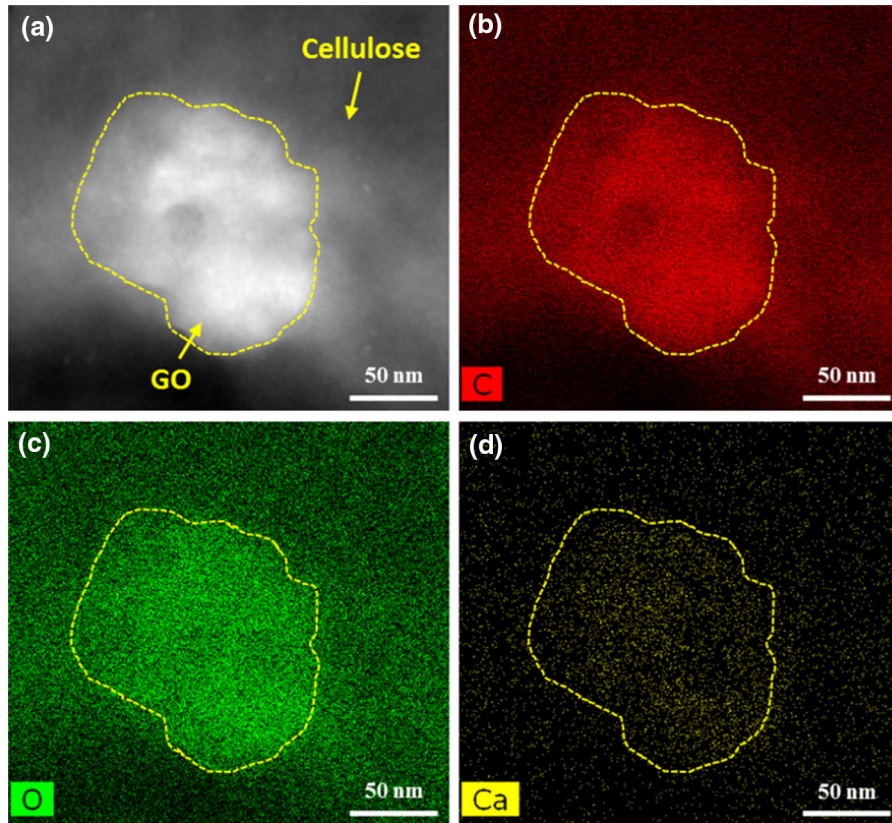


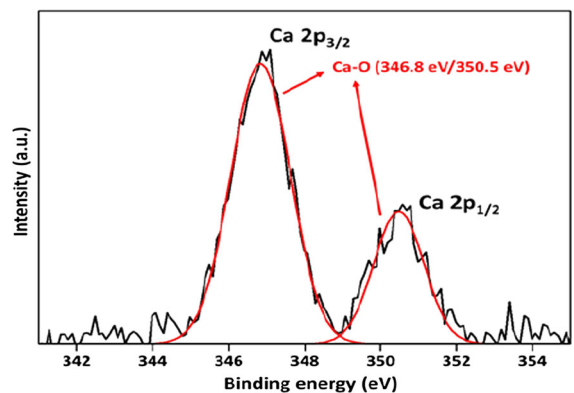
Fig. 7 SEM images of **a** GO/cellulose composite fiber, **b** GO-Ca²⁺-CeHFs

Table 2 Liner density and diameter of GO/Cellulose fiber and various ion-treated fibers

	GO-Cell	Mg	Cu	Fe	Ca	Ba
Linear density (tex)	0.23 ± 0.06	0.22 ± 0.04	0.20 ± 0.07	0.24 ± 0.04	0.23 ± 0.03	0.24 ± 0.04
Diameters (μm)	13.8 ± 0.8	13.4 ± 0.5	12.9 ± 0.8	12.8 ± 0.5	13.7 ± 0.3	13.9 ± 0.5

**Fig. 8** a STEM HAADF images and b–d EDS element mapping images of GO–Ca²⁺–CeHFs (b-carbon; c-oxygen; d-calcium)

treated with Group 2 metal ions (magnesium, calcium, and barium) for 30 min. The graphs indicate that the tensile strength increases in the order of 515 ± 36.4 , 551 ± 37.5 , and 579 ± 24.9 MPa, for magnesium, calcium, and barium treated samples, respectively. The breaking elongation results, on the other hand, are similar for all three samples ($\sim 5.7\%$). The graphs in Fig. 10b illustrate the results from samples treated with Period 4 elements (calcium, copper, and iron) for 30 min. The tensile strengths for copper, iron, and calcium treated samples were 500 ± 57.3 , 507 ± 35.9 , and 551 ± 37.5 MPa, respectively; likewise, elongations were similar across all samples ($\sim 5.8\%$).

**Fig. 9** De-convoluted Ca XPS spectra of GO–Ca²⁺–CeHFs sample

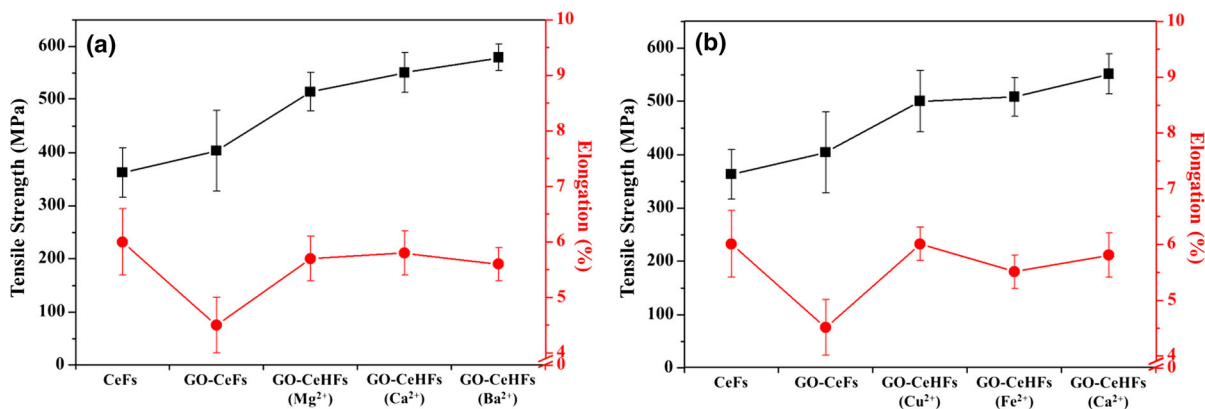


Fig. 10 Tensile strength and elongation of GO–CeHFf after post-treatment via metal ions of **a** group 2 and **b** period 4 in the periodic table

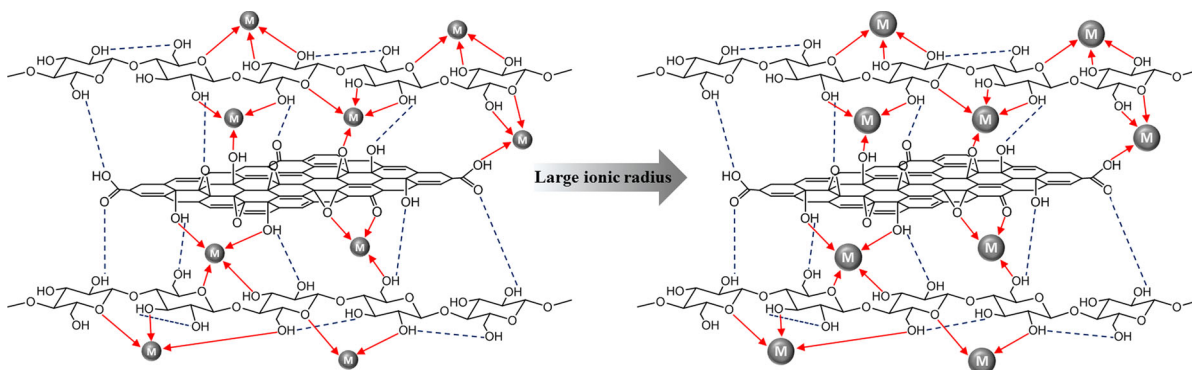


Fig. 11 Schematic description of the reaction between functional groups and metal ions (M) having different ionic radius in the GO–CeHFf after post treatment

Table 3 Ionic radii of cation used in the experiment

Cation	Mg ²⁺	Cu ²⁺	Fe ²⁺	Ca ²⁺	Ba ²⁺
Ionic radius (Å)	0.65	0.70	0.75	0.99	1.34

These results can be interpreted in terms of the size of the ionic radius. The larger the size of the ionic radius, the more space is filled at the interface between the cellulose and GO shown at Fig. 11.

Therefore, the infiltration of metal ions with larger radius to the interface can be correlated to the enhancement of mechanical properties (Matos and Arruda 2003; Okieimen et al. 1985; Martell and Hancock 1996; Park et al. 2008). The ionic radius presents in Table 3 (Chao et al. 1984; Faur-Brasquet et al. 2002; Shimada et al. 1992). This is clearly confirmed by post-treated sample with barium (the largest ion tested in this experiment); that is, the tensile

strength of GO–Ba²⁺–CeHFf show the best improvement over the GO–CeFs by 44%.

Conclusion

The key contribution of this study is the development of the concept of graphene reinforced cellulosic fibers with minimum reduction of toughness. The fabricated GO–CeHFf were treated with various metal ions in order to form a strong interfacial bonding between GO and cellulose. The tensile strength of the fibers treated with Ca ions (GO–Ca²⁺–CeHFf) was around 37% higher than that of GO–CeFs. The addition of GO to the fibers recovered 31% of the reduced elongation; thus, the elongation at break was comparable to that of the conventional cellulose. In addition, the tensile strength of each fibers treated with metal ions from

Group 2 and Period 4 were determined. It is observed that the improvements in the tensile strength were correlated to the larger ionic radius of the metal ions; as a result, the barium treated fibers (GO–Ba²⁺–CeHF_s) yielded the tensile strength of 44% higher than that of GO–CeHF_s. Likewise, the tensile strength of GO–Ba²⁺–CeHF_s was about 60% higher than GO–CeHF_s.

Acknowledgments This research was supported by Nano-Material Technology Development Program through the National Research Foundation of Korea funded by the Ministry of Science, ICT and Future Planning (NRF-2016M3A7B4900135).

References

- ASTM D1577-07 (2012) Standard Test Methods for Linear Density of Textile Fibers. ASTM International, West Conshohocken. <https://doi.org/10.1520/D1577-07R12>
- Belgacem MN, Czeremuszkin G, Sapiha S (1995) Surface characterization of cellulose fibres by XPS and inverse gas chromatography. *Cellulose* 2:145–157
- Chao SH, Suzuki Y, Zysk JR, Cheung WY (1984) Activation of calmodulin by various metal cations as a function of ionic radius. *Mol Pharmacol* 26:75–82
- Charleux B, Coperet C, Lacote E (2015) Chemistry of organo-hybrids: synthesis and characterization of functional nano-objects. Wiley, New York
- Chen L, Xu Z, Li J, Zhou B, Shan M, Li Y, Liu L, Li B, Niu J (2014) Modifying graphite oxide nanostructures in various media by high-energy irradiation. *RSC Adv* 4:1025–1031
- Domun N, Hadavinia H, Zhang T, Sainsbury T, Liaghat GH, Vahid S (2015) Improving the fracture toughness and the strength of epoxy using nanomaterials—a review of the current status. *Nanoscale* 7:10294–10329
- Dreyer DR, Park S, Bielawski CW, Ruoff RS (2010) The chemistry of graphene oxide. *Chem Soc Rev* 39:228–240
- Faur-Brasquet C, Reddad Z, Kadirvelu K, Cloirec PL (2002) Modeling the adsorption of metal ions (Cu²⁺, Ni²⁺, Pb²⁺) onto ACCs using surface complexation models. *Appl Surf Sci* 196:356–365
- Feng Y, Zhang X, Shen Y, Yoshino K, Feng W (2012) A mechanically strong, flexible and conductive film based on bacterial cellulose/graphene nanocomposite. *Carbohydr Polym* 87:644–649
- Geim AK, Novoselov KS (2007) The rise of graphene. *Nat Mater* 6:183–191
- Huang FY, Wu XJ, Yu Y, Lu YH (2015) Preparation and properties of cellulose laurate (CL)/starch nanocrystals acetate (SNA) bio-nanocomposites. *Polymers* 7:1331–1345
- Hummers WS Jr, Offerman RE (1958) Preparation of graphitic oxide. *J Am Chem Soc* 80:1339
- Kramar AD, Žekić AA, Obradović BM, Kuraica MM, Kostić MM (2014) Study of interaction between nitrogen DBD plasma-treated viscose fibers and divalent ions Ca²⁺ and Cu²⁺. *Cellulose* 21:3279–3289
- Kudin KN, Ozbas B, Schniepp HC, Prud'homme RK, Aksay IA, Car R (2008) Raman spectra of graphite oxide and functionalized graphene sheets. *Nano Lett* 8:36–41
- Lee SH, Wang S (2006) Biodegradable polymers/bamboo fiber biocomposite with bio-based coupling agent. *Compos A* 37:80–91
- Li W, Dichiaro A, Bai J (2013) Carbon nanotube-graphene nanoplatelet hybrids as high-performance multifunctional reinforcements in epoxy composites. *Compos Sci Technol* 74:221–227
- Li Y, Zhu H, Zhu S, Wan J, Liu Z, Vaaland O, Lacey S, Fang Z, Dai H, Li T, Hu L (2015) Hybridizing wood cellulose and graphene oxide toward high-performance fibers. *NPG Asia Mater* 7:e150
- Liu LH, Métivier R, Wang S, Wang S (2012) Advanced nanohybrid materials: surface modification and applications. *J Nanometer* 2012:1–2
- Martell E, Hancock RD (1996) Metal complexes in aqueous solutions. Plenum Press, New York
- Matos GD, Arruda MAZ (2003) Vermicompost as natural adsorbent for removing metal ions from laboratory effluents. *Process Biochem* 39:81–88
- Mohanty AK, Misra M, Hinrichsen G (2000) Biofibres, biodegradable polymers and biocomposites: an overview. *Macromol Mater Eng* 276–277:1–24
- Okeimen FE, Ogbeifun DE, Nwala GN, Kumsah CA (1985) Binding of cadmium, copper, and lead ions by modified cellulosic materials. *Bull Environ Contam Toxicol* 34:866–870
- Öztürk HB, Manh JV, Bechtold T (2009) Interaction of cellulose with alkali metal ions and complexed heavy metals. *Lenzing Ber* 87:142–150
- Park S, Lee KS, Bozoklu G, Cai W, Nguyen ST, Ruoff RS (2008) Graphene oxide papers modified by divalent ions-enhancing mechanical properties via chemical cross-linking. *ACS Nano* 2:572–578
- Shi H, Li W, Zhong L, Xu C (2014) Methylene blue adsorption from aqueous solution by magnetic cellulose/graphene oxide composite: equilibrium, kinetics, and thermodynamics. *Ind Eng Chem Res* 53:1108–1118
- Shimada K, Fujikawa K, Yahara K, Nakamura T (1992) Antioxidative properties of xanthan on the autoxidation of soybean oil in cyclodextrin emulsion. *J Agric Food Chem* 40:945–948
- Siró I, Plackett D (2010) Microfibrillated cellulose and new nanocomposite materials: a review. *Cellulose* 17:459–494
- Stankovich S, Dikin DA, Dommett GHB, Kohlhaas KM, Zimney EJ, Stach EA, Piner RD, Nguyen ST, Ruoff RS (2006) Graphene-based composite materials. *Nature* 442:282–286
- Terzopoulou Z, Kyzas GZ, Bikiaris DN (2015) Recent advances in nanocomposite materials of graphene derivatives with polysaccharides. *Materials* 8(2):652–683
- Tian M, Qu L, Zhang X, Zhang K, Zhu S, Guo X, Han G, Tang X, Sun Y (2014) Enhanced mechanical and thermal properties of regenerated cellulose/graphene composite fibers. *Carbohydr Polym* 111:456–462
- Unterweger C, Brüggermann O, Fürst C (2014) Synthetic fibers and thermoplastic short-fiber-reinforced polymers: properties and characterization. *Polym Compos* 35:227–236
- Wang JY, Yang SY, Huang YL, Tien HW, Chin WK, Ma CCM (2011) Preparation and properties of graphene oxide/

- polyimide composite films with low dielectric constant and ultrahigh strength via in situ polymerization. *J Mater Chem* 21:13569–13575
- Wang B, Lou W, Wang X, Hao J (2012) Relationship between dispersion state and reinforcement effect of graphene oxide in microcrystalline cellulose-graphene oxide composite films. *J Mater Chem* 22:12859–12866
- Wang S, Jiang F, Xu X, Kuang Y, Fu K, Hitz E, Hu L (2017) Super-strong, super-stiff macrofibers with aligned, long bacterial cellulose nanofiber. *Adv Mater* 29:1702498
- Wu T, Farnood R (2015) A preparation method of cellulose fiber networks reinforced by glutaraldehyde-treated chitosan. *Cellulose* 22:1955–1961
- Xu Z, Sun H, Zhao X, Gao C (2013) Ultrastrong fibers assembled from giant graphene oxide sheets. *Adv Mater* 25:188–193
- Yadav M, Rhee KY, Jung IH, Park SJ (2013) Eco-friendly synthesis, characterization and properties of a sodium carboxymethyl cellulose/graphene oxide nanocomposite film. *Cellulose* 20:687–698
- Yang J, Chen S, Chen Y, Wang B, Pei Q, Wang H (2017) Macrofibers with high mechanical performance based on aligned bacterial cellulose nanofibers. *ACS Appl Mater Interfaces* 9:20330–20339
- Zhao H, Kwak JH, Zhang ZC, Brown HM, Arey BW, Holladay JE (2007) Studying cellulose fiber structure by SEM, XRD, NMR and acid hydrolysis. *Carbohydr Polym* 68:235–241
- Zhbankov RG, Firsov SP, Buslov DK, Nikonenko NA, Marchewha MK, Ratajczak H (2002) Structural physico-chemistry of cellulose macromolecules. Vibrational spectra and structure of cellulose. *J Mol Struct* 614:117–125
- Zhu Y, Murali S, Cai W, Li X, Suk JW, Potts JR, Ruoff RS (2010) Graphene and graphene oxide: synthesis, properties, and applications. *Adv Mater* 22:3906–3924